frontiers | Frontiers in Environmental Science

TYPE Original Research
PUBLISHED 21 October 2022
DOI 10.3389/fenvs.2022.1024795

Check for updates

OPEN ACCESS

EDITED BY
Gen Zhang,
Chinese Academy of Meteorological Sciences, China

REVIEWED BY
Yun Lin,
Joint Institute for Regional Earth System Science and Engineering, College of Physical Sciences, University of California, Los Angeles, United States
Shupeng Zhu,
University of California, Irvine, United States

*CORRESPONDENCE
Wei Tang,
tangwei@craes.org.cn

SPECIALTY SECTION
This article was submitted to Atmosphere and Climate, a section of the journal Frontiers in Environmental Science

RECEIVED 22 August 2022
ACCEPTED 06 October 2022
PUBLISHED 21 October 2022

CITATION
Du X, Tang W, Zhang Z, Chen J, Han L, Yu Y, Li Y, Li Y, Li H, Chai F and Meng F (2022), Responses of ozone concentrations to the synergistic control of NO_x and VOCs emissions in the Chengdu metropolitan area.
Front. Environ. Sci. 10:1024795.
doi: 10.3389/fenvs.2022.1024795

Responses of ozone concentrations to the synergistic control of NO_x and VOCs emissions in the Chengdu metropolitan area

Xiaohui Du[1,2,3], Wei Tang[1]*, Zhongzhi Zhang[1], Junhui Chen[4], Li Han[4], Yang Yu[1], Yang Li[1], Yingjie Li[4], Hong Li[1], Fahe Chai[1] and Fan Meng[2]

[1]Atmospheric Environment Institute, Chinese Research Academy of Environmental Sciences, Beijing, China, [2]State Key Laboratory of Environmental Criteria and Risk Assessment, Chinese Research Academy of Environmental Sciences, Beijing, China, [3]College of Water Sciences, Beijing Normal University, Beijing, China, [4]Sichuan Academy of Environmental Sciences, Chengdu, China

Simulations of 108 emission reduction scenarios for NO_x and VOCs using Comprehensive Air Quality Model with Extensions (CAMx) were conducted for eight cities in the Chengdu metropolitan area (CMA). The isopleth diagrams were drawn to explore the responses and differences of ozone (O_3) concentrations to NO_x and VOCs emission changes under Chengdu, CMA and Sichuan Province emission reduction scenarios. The results show that the O_3-sensitive regimes of eight cities may change under different emission reduction scenarios. Under Chengdu emission reduction scenario, the Chengdu city is in the transition regime and O_3 formation will shift from transition to VOC-limited when the VOCs emissions decreased by 50%, and the decreases in O_3 concentrations caused by VOCs emission reductions are small. For the CMA and Sichuan Province emission reduction scenarios, all cities are NO_x-limited in the baseline cases and with at least a 66% and a 77% reduction in NO_x emissions, respectively, the daily maximum 8-h average O_3 (MDA8) can attain the O_3 standard (160 μg m^{-3}). Although reductions in VOCs emissions can also lessen the O_3 concentration, the effectiveness is relatively small. The changes in O_3 concentrations under different VOCs to NO_x emission reduction ratios indicate that all cities achieve a relatively high O_3 concentration decrement with low VOCs to NO_x emission reduction ratios and that the decreasing O_3 concentrations caused by non-local emission reductions are much higher than those achieved by local emission reductions. In addition, the decreases in O_3 concentrations in Chengdu are quite close when the total NO_x and VOCs emissions reduction percentages are less than 30% under the CMA and Sichuan emission reduction scenarios.

KEYWORDS

ozone modeling, emission reduction scenarios, O3-sensitive regimes, empirical kinetic modeling approach, Chengdu metropolitan area

1 Introduction

High ozone (O_3)concentrations threaten human health and shorten human life (Amann et al., 2008). The mechanism of O_3 formation and destruction is very complex. O_3 can be generated *via* a series of complex chemical reactions between nitrogen oxides (NO_x) and volatile organic compounds (VOCs) under sunlight conditions (Haagen-Smit, 1952; Yu, 2019; Li et al., 2022). Therefore, it is useful to study the relationship between the changes of NO_x and VOCs emissions and O_3 pollution in oreder to develop mitigation strategies that effectively reduce O_3 concentrations. The Chengdu metropolitan area (CMA) has become a large urban agglomeration in southwestern China due to its rapid industrial development and population growth (Yang et al., 2020), leading to a significant increase in air pollutant emissions and air pollution problems (Zhou et al., 2019). O_3 concentrations in CMA have gradually increased from 2015 to 2019. The number of days when the daily maximum 8-h average O_3 concentration (MDA8) in CMA exceeded the secondary standard of the Ambient Air Quality Standard (GB3095-2012) increased by 95 days, and the total number of exceeding days for 2019 reached 331 days in CMA. The number of days with excessive O_3 concentrations in Chengdu accounted for 1/6 of the polluted days in 2019. Therefore, it is essential to control regional O_3 pollution in the CMA region.

Studies show that when NO_x emissions are at very high level, the reaction of NO_x with OH radicals will inhibit the formation of O_3. However, when VOCs emissions increase concurrently, O_3 concentrations increase. At very high VOCs emissions, the rate of self-reaction of HO_2 is much greater than its reaction with NO, and increasing NO_x emissions will enhance O_3 formations as well (Zhang, 2013; Itahashi et al., 2015, 2020; Kim et al., 2017; Wickham et al., 2019). This indicates that the relationships among O_3-NO_x-VOC need to be considered in conjunction with NO_x and VOCs emission reductions to prevent O_3 pollution. The 'Ozone Pollution Prevention and Control Action Program' implemented in 2017 in Chengdu demonstrated that scientific emission reduction ratio of VOCs to NO_x could reduce the O_3 concentration in Chengdu more effectively (Wu and Xie, 2017). Other studies conducted in different regions also revealed that appropriate VOCs to NO_x ratios could enhance the reduction of O_3 concentrations (Chen et al., 2019; He et al., 2019; Wang et al., 2019).

The response of O_3 to NO_x and VOCs emissions can be determined by setting different NO_x and VOCs emissions abatement scenarios to simulate the changes in O_3 concentrations, and the sensitivities of O_3 to VOCs and NO_x emissions can be explored by plotting empirical kinetic modeling approach (EKMA) curves based on various emission reduction scenarios (Qu et al., 2014; Ou et al., 2016; Tan et al., 2018; Cui et al., 2021; Jiang et al., 2021; Liu et al., 2021). Although the contributions from local emissions play an important role in O_3 foramtion in CMA (Yang et al., 2020; Yang et al., 2021), studies investigating the separate effects of local and regional emissions on O_3 concentrations in the CMA region have not been widely conducted.

In this study, 108 emission reduction scenarios for NO_x and VOCs emissions, including 36 scenarios for the Chengdu city, 36 scenarios for the CMA region and 36 scenarios for Sichuan Province are conducted using the Comprehensive Air Quality Model with Extensions (CAMx) model, to explore the different effects of local and regional emissions on O_3 concentrations and to develop a more refined O_3 abatement policy for the Chengdu city. The effects of changes in NO_x and VOCs emissions from different source regions on the O_3 concentrations are compared and discussed. The results provide the scientific supports for developing O_3 control measures at municipal and regional levels in the CMA region.

2 Method and material

2.1 Model description and settings

CAMx, version 7.1 (ENVIRON, 2020), is a third-generation three-dimensional (3D) air quality model and can be applied to multi-scale integrated simulation studies of photochemical smog and fine particulate matter in a 3D nested grid. It can provide several extensions, such as source apportionment techniques, sensitivity analysis, process analysis, *etc.* These extension modules have been widely used in China and abroad (Chatani et al., 2020; A. M. Dunker, 2015; Alan M. Dunker et al., 2015; Yarwood et al., 2013).

In this study, the horizontal resolution of the master grid is 36 × 36 km (Figure 1A), covering the whole China, Northeast Asia and some parts of Southeast Asia. The nested grid is 12 × 12 km, covering Sichuan Province and its surrounding areas (Figure 1B). The model is divided into 20 layers vertically. The Weather Research and Forecasting (WRF v3.9.1.1) model (Skamarock et al., 2019) is used to provide meteorological conditions, with the input data (6 h interval) from the National Centers for Environmental Prediction (NCEP) Final Analysis (FNL). The gas-phase chemical mechanism is SAPRC07 and the coarse/fine aerosol chemistry scheme is used for the aerosol chemistry mechanism. The photolysis rates used in the model are calculated using the O_3 column concentrations from the Ozone Monitoring Instrument (OMI) data.

The emissions inventory for the master grid (36 km) is based on the Multi-resolution Emission Inventory for China (MEIC 2016, Li et al., 2017) and Regional Emission Inventory in Asia (REAS2.1, Kurokawa et al., 2013). The emission inventory used for the nest grid (12 km) is according to MEIC2016 and adjusted by the localized air pollutant emission inventory. VOCs emission is subdivided into 116 species using the VOCs species consolidation methods

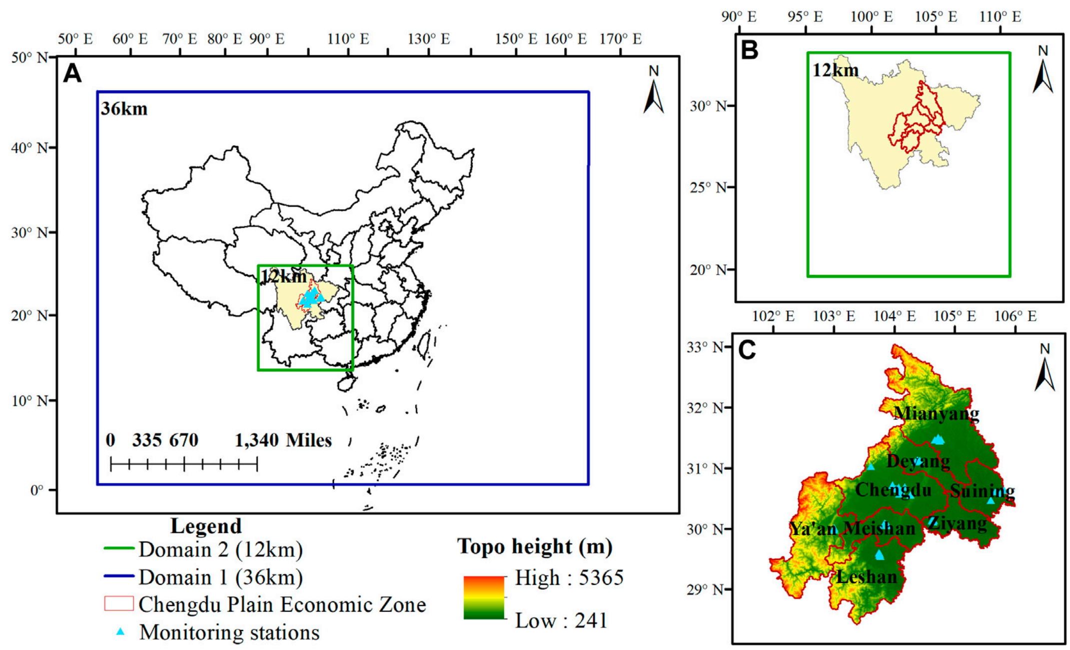

FIGURE 1
Modeling domains for **(A)** East Asia, **(B)** Sichuan and its surrounding area and **(C)** the CMA region. The blue triangles in (C) represent national air quality monitoring stations.

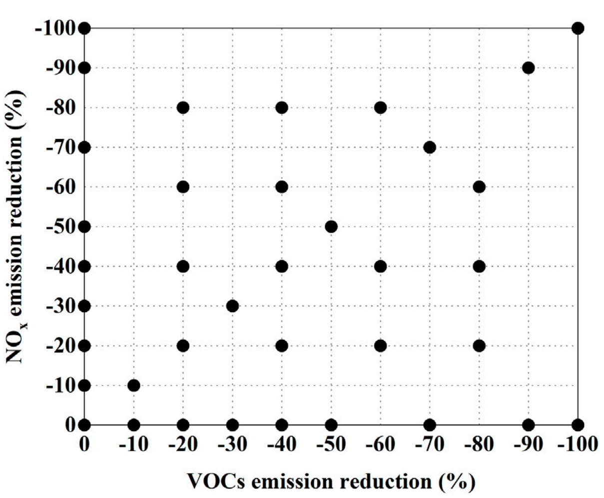

FIGURE 2
NOx and VOCs emission reductions matrix.

introduced by Carter. (2000), Li et al. (2014) and Carter and Heo. (2013) for allocation of VOCs species for the SAPRC07 mechanism. The biogenic emissions used in the simulations are generated by the Model of Emissions of Gases and Aerosols from Nature (MEGANv3.1; Guenther et al., 2019).

2.2 Simulation scenarios design

One baseline scenario and 108 emission reduction scenarios are designed in this study. Of the 108 scenarios, 36 are region-wide NO_x and VOCs emissions reductions for Chengdu with emissions outside Chengdu remaining unchanged; 36 are region-wide emission reduction scenarios for eight cities in the CMA region (Chengdu, Deyang, Mianyang, Meishan, Leshan, Ziyang, Suining and Ya'an) with emissions outside CMA remaining unchanged; 36 are region-wide emission reduction scenarios for entire Sichuan Province with emissions outside Sichuan Province remaining unchanged. Figure 2 shows the matrix of different NO_x and VOCs emission reductions. The origin (x = y = 0) represents the baseline scenario and the dots identify the proportions of NO_x and VOCs emissions reduction percentages that are applied for Chengdu, CMA and Sichuan Province. Referring to Ou et al. (2016), Chen et al. (2019) and Luo et al. (2021) for the setting of emission reduction scenarios, since those nearest the baseline cases represent more feasible emissions reductions, the emissions reduction percentages are spaced at 10% intervals when the emissions reduction percentages are 50% or less and at 20% intervals when the emissions reduction percentages exceeded 50%. In order to investigate the changes in O_3 concentrations at different emissions reduction ratios of VOCs to NO_x, 12 scenarios with different reduction percentages of NO_x and VOCs emissions are designed (e.g., 20% reduction for NO_x and 40% reduction for VOCs). All simulations are conducted for the August

TABLE 1 Comparisons of observed and simulated MDA8 O_3 concentrations on polluted days in eight cities in August 2019 (MDA8 O_3 concentrations exceeding 160 μg m^{-3}).

City name	Observed MDA8 O_3	Simulated MDA8 O_3	Fractional bias (%)	Number of pollution days
Chengdu	194.64	175.42	−10.80	14
Deyang	209.14	179.11	−14.09	7
Leshan	177.50	199.99	12.12	6
Meishan	188.00	182.30	−3.55	10
Mianyang	179.17	171.52	−5.52	6
Suining	179.43	223.51	21.59	7
Ya'an	170.00	167.54	−1.93	4
Ziyang	178.33	193.49	6.63	9

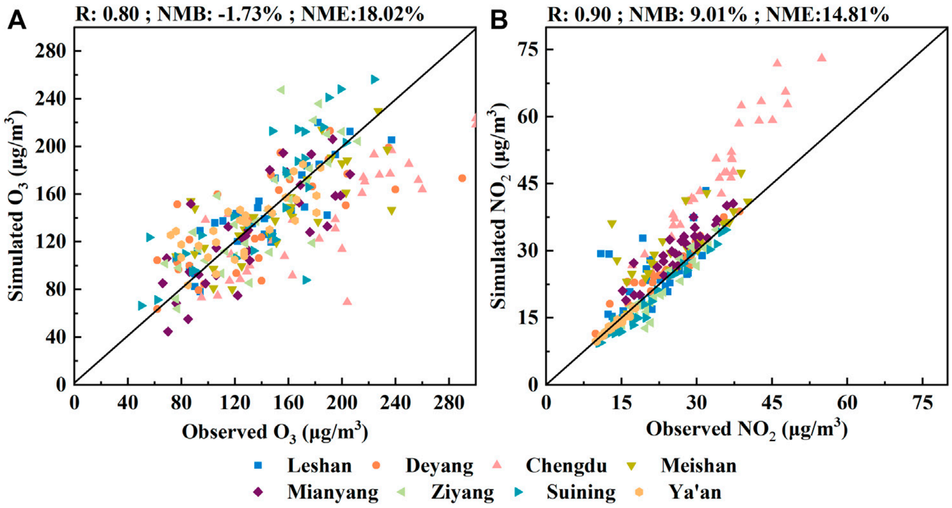

FIGURE 3
Comparisons of **(A)** daily maximum 8-h average O_3 and **(B)** daily averaged NO_2 concentrations in eight cities of the CMA region in August 2019.

2019 period, and the other input parameters used for all simulations are unified. Finally, the responses of O_3 to NO_x and VOCs emission reductions are calculated based on the 108 emission reduction scenarios and are visualised *via* O_3-NO_x-VOC isopleths.

Considering that pollution control measures are mainly targeted at stages of heavy pollution, O_3 polluted days in each city are selected as those for which the observed and simulated MDA8 O_3 concentrations are simultaneously greater than 160 μg m^{-3}, and the number of O_3 polluted days during August 2019 are counted (Table 1), the simulated MDA8 O_3 concentrations for each city are averaged over the modeling grids where the monitoring stations are located. The factional bias between observed and simulated MDA8 O_3 concentrations are calculated for each city, showing that the model is well performed for simlulating the polluted days with most of biases less than 20%.

3 Results and discussions

3.1 Model evaluation

The evaluation of the model performance for O_3 and NO_2 concentrations in cities of the CMA region is illustrated in Figure 3. The observed MDA8 O_3 concentrations and the daily NO_2 concentrations averaged over the monitoring sites in each city are used against the simulated data. The simulated MDA8 O_3 concentrations in August 2019 are extracted from the modeling grids where the monitoring stations are located. A total of 37 national monitoring stations in the eight cities in CMA are chosen for model validations (Figure 1C). The statistical metrics, correlation coefficient (R), normalised mean bias (NMB) and normalised mean error (NME) show that the correlations between simulated and observed O_3 and NO_2 concentrations

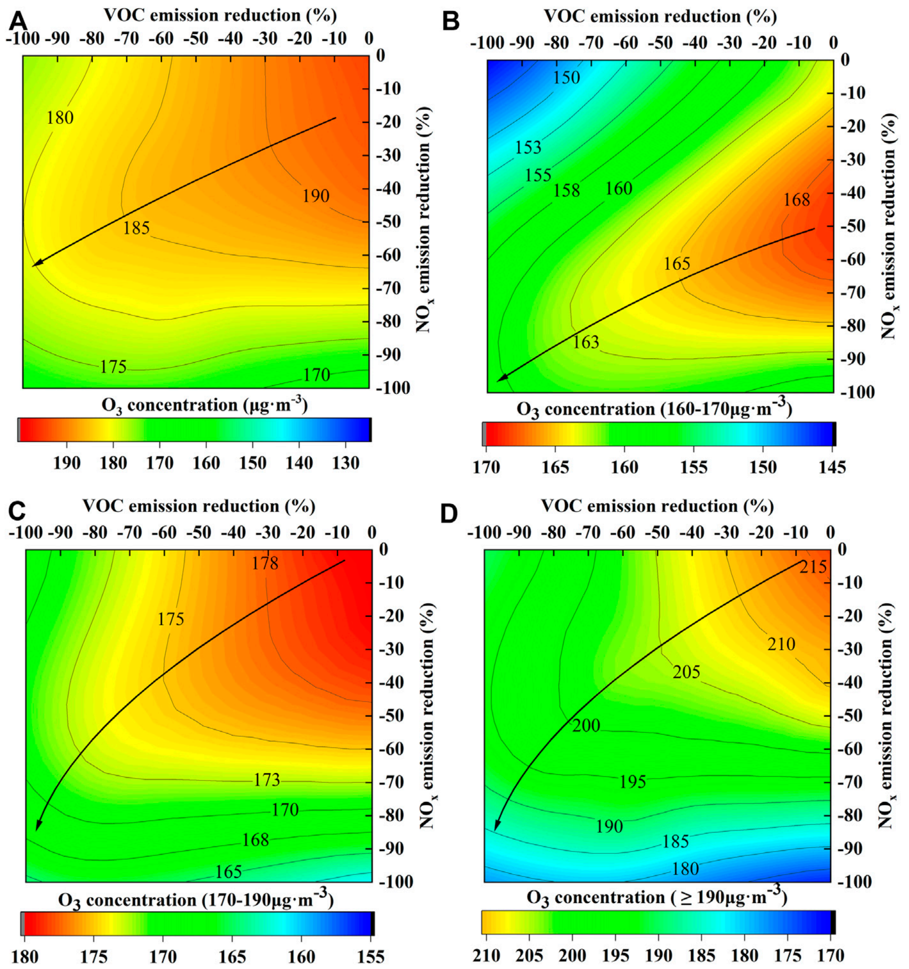

FIGURE 4
Isopleth diagrams of MDA8 O_3 varing with VOCs and NO_x emission reductions in Chengdu for **(A)** all polluted days, **(B)** polluted days with MDA8 O_3 concentrations in the range of 160–170 μg m^{-3}, **(C)** polluted days with MDA8 O_3 concentrations in the range of 170–190 μg m^{-3} and **(D)** polluted days with MDA8 O_3 concentrations greater than 190 μg m^{-3} (the black arrows are ridgelines).

are both greater than 0.8, the NMB values of O_3 and NO_2 are −1.73% and 9.01%, and the NME values of O_3 and NO_2 are 18.02% and 14.81%, indicating that the model generally performs well over the CMA region (Emery et al., 2017).

3.2 Responses of O_3 to NO_x and VOCs emission reductions

3.2.1 Reduction scenarios in chengdu

A baseline and thirty-six abatement scenarios were conducted to investigate the effects of local and regional emission reductions on MDA8 O_3 concentrations in Chengdu. Isopleth diagrams of average MDA8 O_3 concentration are plotted on polluted days during August 2019 with NO_x and VOCs emissions reduced only for Chengdu (Figure 4A), following the method as described in Section 2.2 (Table 1). The decreases in O_3 concentrations due to the reductions of local NO_x and VOCs emissions for Chengdu are small, even with a 100% reduction of local emissions, which only brings down the MDA8 O_3 concentration close to 170 μg m^{-3}. The isopleth diagrams illustrate that the MDA8 O_3 concentration for the baseline scenario is skewed towards the transition regime (Figure 4A). When the VOCs emissions gradually reduce and NO_x emissions remain the same or decrease less than the VOCs emissions, the O_3-sensitive regime in Chengdu gradually moves toward VOC-limited.

The average MDA8 O_3 polluted days during August 2019 in Chengdu are divided into three categories based on the following concentration ranges, 160–170 μg m^{-3}, 170–190 μg m^{-3} and ≥190 μg m^{-3} (Figures 4B–D). When the MDA8 O_3 concentrations at the range of 160–170 μg m^{-3}, Chengdu is in VOC-limited regime and a decrease in NO_x emissions enhancing

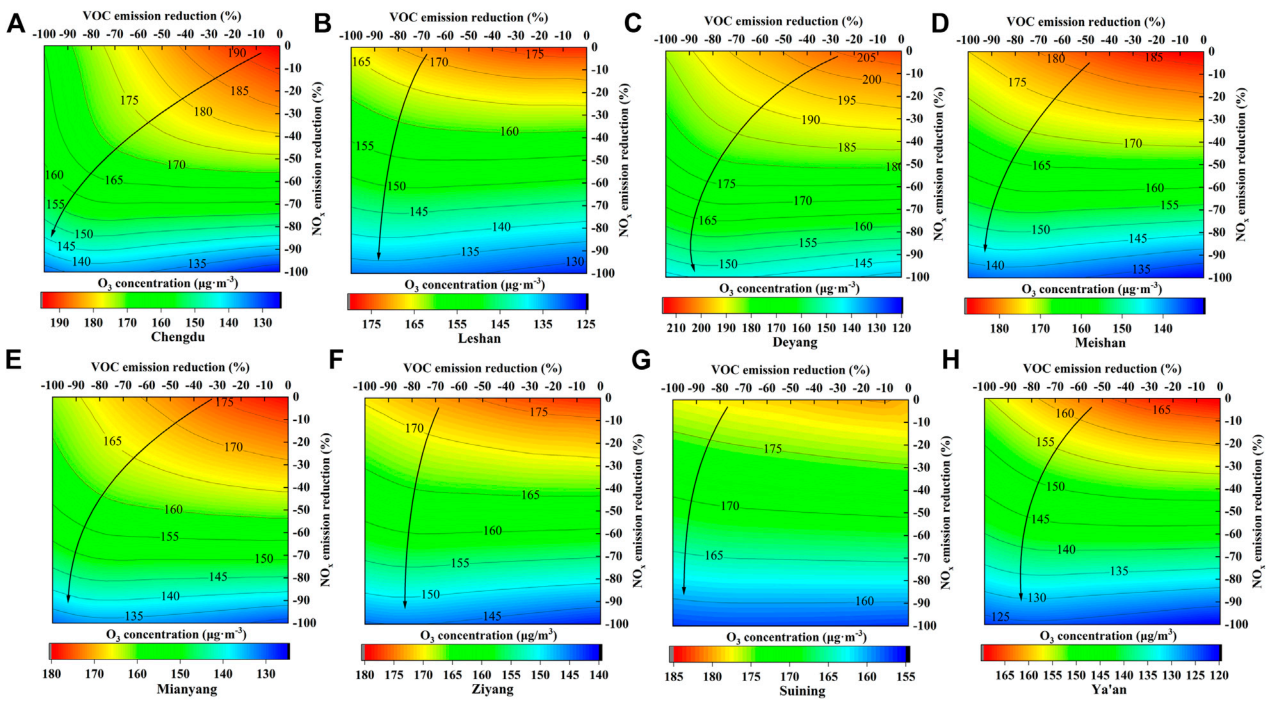

FIGURE 5
Isopleth diagrams of MDA8 O_3 varing with VOCs and NO_x emission reductions for the CMA scenario (**(A)** Chengdu, **(B)** Leshan, **(C)** Deyang, **(D)** Meishan, **(E)** Mianyang, **(F)** Ziyang, **(G)** Suining, **(H)** Ya'an; the black lines with arrows are ridgelines).

O_3 concentrations. However, a 20% reduction in VOCs emissions in Chengdu can bring down the MDA8 O_3 concentration to 160 μg m^{-3}. When the MDA8 O_3 concentration above 170 μg m^{-3}, Chengdu is in a transition regime. At the range of 170–190 μg m^{-3}, MDA8 O_3 concentrations in Chengdu are only likely to reach 160 μg m^{-3} when NO_x emissions decreased by almost 100%. At the O_3 level above 190 μg m^{-3}, the MDA8 O_3 concentrations in Chengdu cannot reach 160 μg m^{-3} if only local emissions are reduced. It indicates that at light levels of O_3 pollution, reducing local emission can attain O_3 standard, while at more severe levels of O_3 pollution, considering regional control measures are necessary in Chengdu.

3.2.2 Reduction scenarios in CMA

In the emission reduction scenario for eight cities in CMA, the isopleth diagrams of MDA8 O_3 illustrates that all cities are mainly NO_x-limited in the baseline scenario except for Chengdu, which is in a transition regime (Figure 5). In Chengdu, the reduction of both NO_x and VOCs emissions resulted in a decrease in O_3 concentration. When NO_x and VOCs emission reductions exceeded 40%, the gradient of O_3 concentration decrement caused by NO_x reduction is greater than that from VOCs reduction. Similar trend is also observed for Deyang. The O_3 isopleths for Leshan, Meishan, Mianyang and Ya'an show that the effects of VOCs emission reductions on O_3 concentrations are small, with only a decrease of O_3 concentration around 5 μg m^{-3} by more than 50% reductions. The nearly horizontal contours of Suining and Ziyang indicate that these two cities are NO_x-limited and reducing NO_x emissions inhibits O_3 formations. Therefore, priorly reducing NO_x emissions in the eight cities of CMA will bring down O_3 concentrations more effectively.

The responses of O_3 concentrations to NO_x and VOCs emissions vary in different cities in the CMA region. The averaged MDA8 O_3 concentrations in cities such as Leshan, Mianyang and Ya'an can attain the standard (160 μg m^{-3}) when NO_x emissions in CMA are reduced by 22–53%. Cities such as Chengdu, Ziyang, Deyang and Meishan need to reduce NO_x emissions in CMA by 60–77% to reach the standard. Although the MDA8 O_3 concentrations in Suining are lower than most of the other cities, the reduction of NO_x emissions in CMA causes a small gradient in the decrease of O_3, resulting in more than 89% reduction of NO_x emissions in CMA to lower down O_3 concentrations below 160 μg m^{-3}. It indicates that synergistic precursor emission reductions from the CMA region or outside CMA are required to achieve more effective O_3 controls.

3.2.3 Reduction scenarios in Sichuan Province

Isopleth diagrams of the averaged MDA8 O_3 concentrations *versus* the VOCs and NO_x emission reduction percentages for

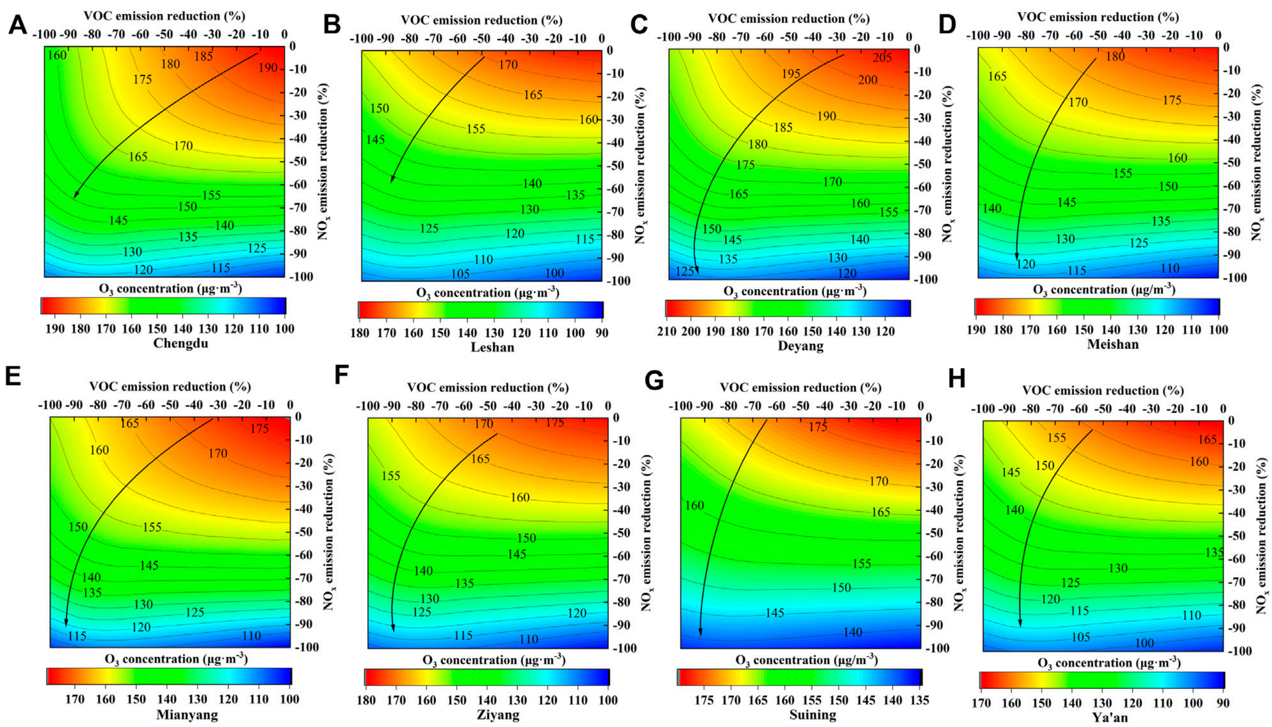

FIGURE 6
Isopleth diagrams of MDA8 O_3 varing with VOCs and NO_x emission reductions for the Sichuan Province scenario (**(A)** Chengdu, **(B)** Leshan, **(C)** Deyang, **(D)** Meishan, **(E)** Mianyang, **(F)** Ziyang, **(G)** Suining, **(H)** Ya'an; the black lines with arrows are ridgelines).

Sichuan Province are shown in Figure 6. It shows that reducing NO_x and VOCs emissions in Sichuan Province cause a larger gradient in the decrease of MDA8 O_3 concentrations compared to those shown in Figure 4 and Figure 5. Although the responses of O_3 concentrations to NO_x and VOCs emissions in most cities are NO_x-limited, the same percentage of VOCs emission reductions in Figure 6 causes a greater decrease in MDA8 O_3 concentrations than in Figure 4 and Figure 5. In Leshan, Mianyang and Meishan, around 30% VOCs emission reductions result in a 5 μg m^{-3} decrease in the O_3 concentrations. Similarly, the MDA8 O_3 concentrations in eight cities reach the 160 μg m^{-3} much faster in the emission reduction scenarios for Sichuan Province. Cities such as Ziyang, Suining, Leshan, Mianyang and Ya'an, NO_x emissions dropped by around 20–45%, and cities such as Chengdu, Deyang and Meishan, NO_x emissions dropped by approximately 48–66%, respectively, MDA8 O_3 concentrations can attain the standard of 160 μg m^{-3}.

The effects of NO_x and VOCs emission reductions from different regions on O_3 concentrations vary significantly among cities. Figure 7 shows the maximum decrements in MDA8 O_3 concentrations for each city under the 100% NO_x and VOCs emission reductions for the CMA region and Sichuan Province. The emission reductions for Sichuan Province result in a maximum decrease in MDA8 O_3 concentrations above 77.4 μg m^{-3} (40%) for most cities, with a maximum of approximately 83.9 μg m^{-3} (47%) in Leshan. The exception is in Suining, which has the smallest decrease in O_3 concentrations among these cities, with a maximum decrease of about 44 μg m^{-3} (25%) in two different regional emission reduction scenarios. A study by Lu et al. (2019) revealed that the background O_3 concentrations from May to August accounted for approximately 50.3% of total O_3 concentrations in the Sichuan Basin, indicating that a 100% reduction of anthropogenic emissions in Sichuan Province may cause less than 50% decrease of total O_3 concentrations.

The maximum decrease in O_3 concentrations in Deyang and Chengdu under the CMA emission reduction scenario is around 71.4 μg m^{-3} (34.1%) and 68.8 μg m^{-3} (35.4%), respectively, and the maximum decrease in O_3 concentrations in Chengdu and Deyang under the Sichuan Province emission reduction scenario is about 97.5 μg m^{-3} (46.6%) and 91.0 μg m^{-3} (46.8%), respectively. The decreases in O_3 concentrations under the Sichuan Province emission reduction scenario are approximately 12% larger compared to the CMA emission reduction scenario, especially in Leshan, Mianyang and Ziyang, decreases in O_3 concentrations under the Sichuan

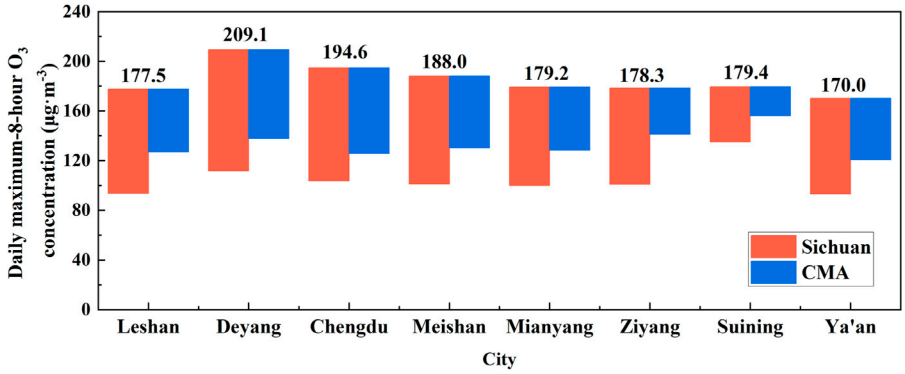

FIGURE 7
The effects of 100% NO_x and VOCs emission reductions on MDA8 O_3 concentrations in eight cities for the CMA and Sichuan Province scenarios.

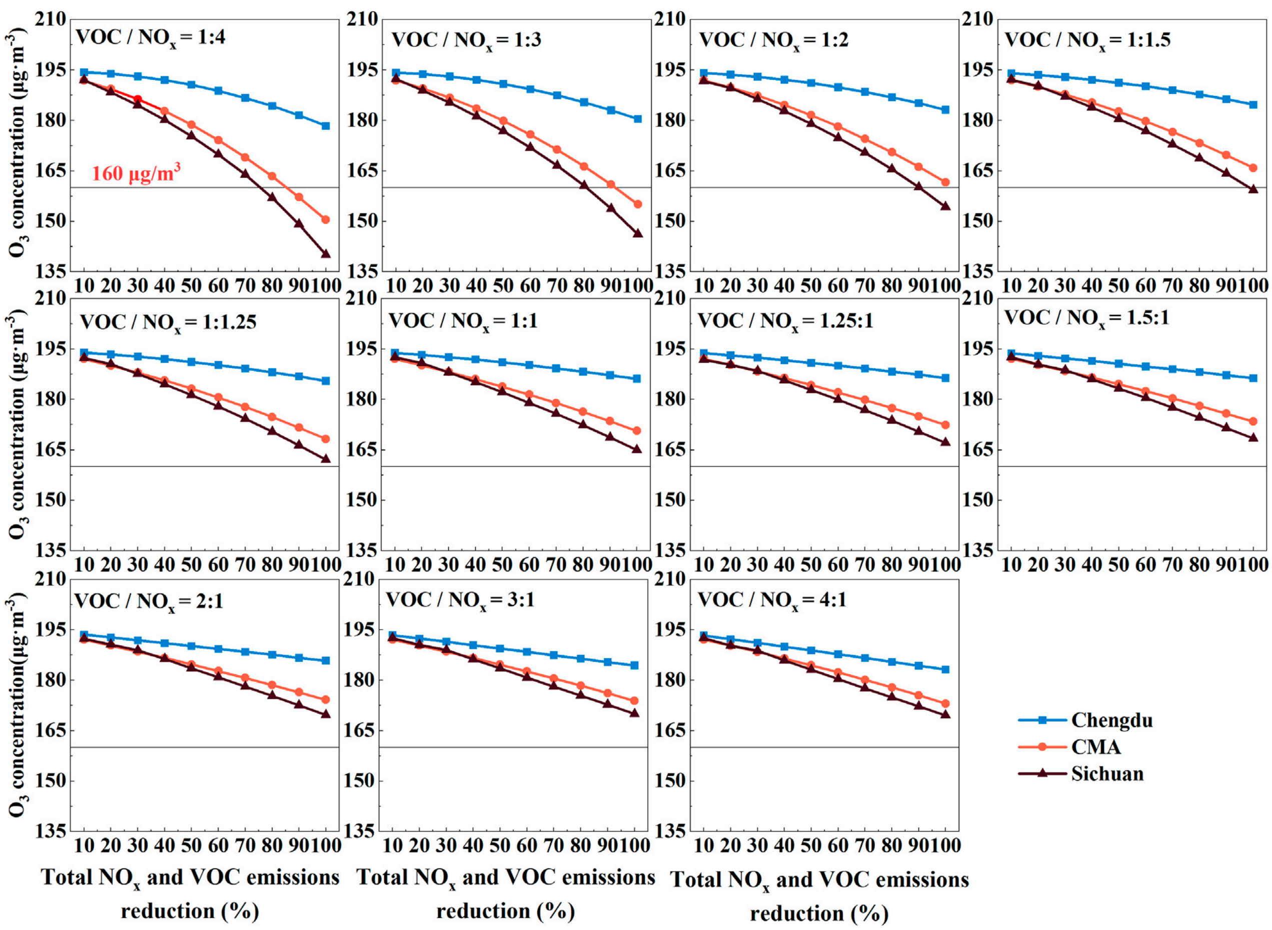

FIGURE 8
Effects of the emission reductions with different VOCs to NO_x ratios on the changes in MDA8 O_3 concentrations under Chengdu, CMA and Sichuan Province scenarios.

Province emission reduction scenario are about 20% higher than those under the CMA emission reduction scenario.

3.3 Differences in O_3 reduction effectiveness

Figures 4–6 illustrate the effects of local and regional emission perturbations on O_3 concentrations. Comparing the O_3 isopleth diagrams for Chengdu, CMA and Sichuan Province emission reduction scenarios reveals that, although the baseline scenario showing Chengdu is in a VOC-limited regime, the reductions of local VOCs emissions have small impact on the decrease of O_3 concentrations. When local VOCs emissions decreased by 60%, the decrease of O_3 concentrations in Chengdu is less than $5\ \mu g\ m^{-3}$. In contrast, under emission reduction scenarios for the CMA and Sichuan Province, to achieve a $5\ \mu g\ m^{-3}$ decrease in MDA8 O_3 concentrations in Chengdu only required a reduction of NO_x or VOCs emissions of less than 20%, and even a smaller reduction rate is demanded if both NO_x and VOCs emissions are reduced. It indicates that the regional and transported emission sources on O_3 concentrations should be considered in emission control strategies.

Referring to the emission ratios of VOCs to NO_x in other studies (Chen et al., 2019; Wang et al., 2019; Yao et al., 2021), 11 different emission reduction ratios of VOCs to NO_x emissions (VOCs/NO_x = 1:4, 1:3, 1:2, 1:1.5, 1:1.25, 1:1, 1.25:1, 1.5:1, 2:1, 3:1, 4:1) within 100% emission reductions under Chengdu, CMA, and Sichuan Province scenarios are conducted to investigate the changes for MDA8 O_3 in Chengdu (Figure 8). When the emission reduction ratio of VOCs/NO_x is greater than 1, the decreasing trend of the averaged MDA8 O_3 concentration is closer to linear and the decrement in the averaged MDA8 O_3 concentration is significantly smaller than those when the ratio is less than 1. In contrast, the decreasing trend in the averaged MDA8 O_3 concentration is non-linear when the emission reduction ratio of VOCs/NO_x is equal to or less than one and the smaller the ratio (the larger reduction of NO_x emission) the faster the O_3 decrease. The largest decrease in the averaged MDA8 O_3 concentration is at the VOCs/NO_x ratio of 1:4.

Among the emission reduction scenarios in different regions, the decrease in the averaged MDA8 O_3 concentration under the Chengdu emission reduction scenario is significantly smaller than those under the other two regional emission reduction scenarios (the CMA and Sichuan Province). However, when the total VOCs and NO_x emission reductions are less than 30%, especially at high ratio of VOCs/NO_x, the decrease in the averaged MDA8 O_3 concentration under these two emission reduction scenarios is almost identical.

4 Conclusion

108 scenarios of NO_x and VOCs emission reductions for different regions were simulated using the CAMx model and the relationship among O_3-NO_x-VOC was obtained in this study. The responses of O_3 formation to the changes in NO_x and VOCs emissions in the CMA region were demonstrated by the O_3 isopleth diagrams. In addition, 11 emission reduction cases with different VOCs-to-NO_x ratios were investigated to explore the changes in O_3 concentrations under different reduction ratios of precursor emissions.

It was found that the O_3-sensitive regimes in Chengdu city was in a transition zone, while the other cities in the CMA region were in the NO_x-limited zone. Eight cities could meet the MDA8 O_3 concentration standard when NO_x emissions in the CMA region were reduced by 77% or more. However, if only cut VOCs emissions, even with a 100% reduction, it failed to attain O_3 standard of $160\ \mu g\ m^{-3}$ for all cities in the CMA region. The results showed that under the NO_x and VOCs emission reduction scenario in Sichuan Province, the most effective way to reduce the peak MDA8 O_3 concentration was to control NO_x emissions, with a 66% reduction in NO_x emissions enabling cities in the CMA region to reach the MDA8 O_3 standard ($160\ \mu g\ m^{-3}$). However, in reality, it is quite difficult to achieve 66% NO_x emission reductions in a short time period. Hence, in order to reach the MDA8 O_3 standard in all cities in the CMA region, joint regional pollutant prevention and control abatement measures outside of Sichuan Province may need to be considered. Although a decrease in VOCs emissions could also reduce the MDA8 O_3 concentration, the effects were smaller than that achieved with a decrease in NO_x emissions, and cutting VOCs emissions alone may not be able to achieve the MDA8 O_3 standard in some cities, such as Deyang, Meishan, and Suining. Overall, the NO_x and VOCs emission reductions in Sichuan Province could reach a 50% higher O_3 concentration decrease than the emission reductions in the CMA region, such as in the Ziyang city, but the other cities such as Deyang, Chengdu and Suining, such differences were not significant.

The MDA8 O_3 concentration decreases resulting from different VOCs to NO_x emission reduction ratios for the eight cities in the CMA region showed that all cities reach higher MDA8 O_3 decreases due to NO_x emissions control. In addition, the effects of non-local emission reductions on MDA8 O_3 decreases were much higher than those from local emission reductions. Furthermore, in the emission reduction scenarios for the CMA and Sichuan Province, the decreases in MDA8 O_3 were almost identical for NO_x and VOCs emission reductions at less than 30%, suggesting that if the non-local NO_x and VOCs emission reductions were small, effects of expanding the emission control area from CMA to Sichuan Province on MDA8 O_3 were insignificant.

O_3 is highly transportable and biogenic VOCs emissions were relatively high in summer, contributing high background O_3 concentrations and increasing the difficulties in O_3 control. Although most cities in the CMA region were NO_x-limited on the regional basis, the synergistic control of NO_x and VOCs emissions was still an effective way to reduce O_3 concentrations in the short term. On the other hand, persistently controlling regional NO_x emissions should become a control measure in a long run to further reduce O_3 levels regionally.

Data availability statement

The raw data supporting the conclusions of this article will be made available by the authors, without undue reservation.

Author contributions

XD and WT contributed significantly to the conception of the study and to model data analysis and manuscript preparation; ZZ, YY and YL conducted simulations and model performance evaluations; JC, LH, YL prepared emission inventory for the modeling; HL, FC and FM helped perform the analysis with constructive discussions. All authors contributed to the article and approved the submitted version.

Funding

This work was supported by National Key Research and Development Project (NO. 2017YFC0213003, NO. 2018YFC0213504, NO. 2016YFC0208905).

Acknowledgments

The authors would like to thank Jiemeng Bao and Zhenhai Wu for providing measurement data.

Conflict of interest

The authors declare that the research was conducted in the absence of any commercial or financial relationships that could be construed as a potential conflict of interest.

Publisher's note

All claims expressed in this article are solely those of the authors and do not necessarily represent those of their affiliated organizations, or those of the publisher, the editors and the reviewers. Any product that may be evaluated in this article, or claim that may be made by its manufacturer, is not guaranteed or endorsed by the publisher.

References

Amann, M., Derwent, D., Forsberg, B., Hanninen, O., Hurley, F., Krzyzanowski, M., et al. (2008). *World Health Organization: Health risks of ozone from long-range transboundary air pollution*. Geneva, Switzerland: World Health Organisation Regional Office for Europe. Available at: http://www.euro.who.int/__data/assets/pdf_file/0005/78647/E91843.pdf (Accessed October 18, 2017).

Carter, W. P. L., and Heo, G. (2013). Development of revised SAPRC aromatics mechanisms. *Atmos. Environ.* 77, 404–414. doi:10.1016/j.atmosenv.2013.05.021

Carter, W. P. L. (2000). Implementation of the saprc-99 chemical mechanism into the models-3 framework. Report, 1–101.

Chatani, S., Shimadera, H., Itahashi, S., and Yamaji, K. (2020). Comprehensive analyses of source sensitivities and apportionments of PM_{2.5} and ozone over Japan via multiple numerical techniques. *Atmos. Chem. Phys.* 20 (17), 10311–10329. doi:10.5194/acp-20-10311-2020

Chen, X., Situ, S., Zhang, Q., Wang, X., Sha, C., Zhouc, L., et al. (2019). The synergetic control of NO2 and O3 concentrations in a manufacturing city of southern China. *Atmos. Environ.* 201 (2), 402–416. doi:10.1016/j.atmosenv.2018.12.021

Cui, M., An, X., Xing, L., Li, G., Tang, G., He, J., et al. (2021). Simulated sensitivity of ozone generation to precursors in beijing during a high O3 episode. *Adv. Atmos. Sci.* 38 (7), 1223–1237. doi:10.1007/s00376-021-0270-4

Dunker, A. M., Koo, B., and Yarwood, G. (2015). Source apportionment of the anthropogenic increment to ozone, formaldehyde, and nitrogen dioxide by the path-integral method in a 3D model. *Environ. Sci. Technol.* 49 (11), 6751–6759. doi:10.1021/acs.est.5b00467

Dunker, A. M. (2015). Path-integral method for the source apportionment of photochemical pollutants. *Geosci. Model Dev.* 8 (6), 1763–1773. doi:10.5194/gmd-8-1763-2015

Emery, C., Liu, Z., Russell, A. G., Odman, M. T., Yarwood, G., and Kumar, N. (2017). Recommendations on statistics and benchmarks to assess photochemical model performance. *J. Air Waste Manag. Assoc.* 67 (5), 582–598. doi:10.1080/10962247.2016.1265027

ENVIRON (2020). *CAMx (comprehensive air quality model with extensions) user's guide version 7.10*. Novato, CA: ENVIRON International Corporation.

Guenther, A., Jiang, X., Shah, T., Huang, L., Kemball-Cook, S., and Yarwood, G. (2019). "Model of emissions of gases and aerosol from nature version 3 (MEGAN3)," in *Air pollution modeling and its application XXVI* (Cham: Springer), 187.

Haagen-Smit, A. J. (1952). Chemistry and physiology of Los Angeles smog. *Ind. Eng. Chem.* 44 (6), 1342–1346. doi:10.1021/ie50510a045

He, Z., Wang, X., Ling, Z., Zhao, J., Guo, H., Shao, M., et al. (2019). Sources of methacrolein and methyl vinyl ketone and their contributions to methylglyoxal and formaldehyde at a receptor site in Pearl River Delta. *J. Environ. Sci.* x, 1–10. doi:10.1016/j.jes.2018.12.001

Itahashi, S., Hayami, H., and Uno, I. (2015). Comprehensive study of emission source contributions for tropospheric ozone formation over East Asia. *J. Geophys. Res. Atmos.* 120 (1), 331–358. doi:10.1002/2014JD022117

Itahashi, S., Mathur, R., Hogrefe, C., Napelenok, L. S., and Zhang, Y. (2020). Modeling stratospheric intrusion and trans-Pacific transport on tropospheric ozone using hemispheric CMAQ during April 2010 - Part 2: Examination of emission impacts based on the higher-order decoupled direct method. *Atmos. Chem. Phys.* 20 (6), 3397–3413. doi:10.5194/acp-20-3397-2020

Jiang, Z., Shi, H., Zhao, B., Gu, Y., Zhu, Y., Miyazaki, K., et al. (2021). Modeling the impact of COVID-19 on air quality in southern California: Implications for future control policies. *Atmos. Chem. Phys.* 21 (11), 8693–8708. doi:10.5194/acp-21-8693-2021

Kim, E., Kim, B. U., Kim, H. C., and Kim, S. (2017). The variability of ozone sensitivity to anthropogenic emissions with biogenic emissions modeled by MEGAN and BEIS. *Atmosphere* 8 (10), 187–225. doi:10.3390/atmos8100187

 10.3389/fenvs.2022.1024795

Kurokawa, J., Ohara, T., Morikawa, T., Hanayama, S., Janssens-Maenhout, G., Fukui, T., et al. (2013). Emissions of air pollutants and greenhouse gases over Asian regions during 2000–2008: Regional Emission inventory in Asia (REAS) version 2. *Atmos. Chem. Phys.* 13 (21), 11019–11058. doi:10.5194/acp-13-11019-2013

Li, M., Liu, H., Geng, G., Hong, C., Liu, F., Song, Y., et al. (2017). Anthropogenic emission inventories in China: A review. *Natl. Sci. Rev.* 4 (6), 834–866. doi:10.1093/nsr/nwx150

Li, M., Zhang, Q., Streets, D. G., He, K. B., Cheng, Y. F., Emmons, L. K., et al. (2014). Mapping Asian anthropogenic emissions of non-methane volatile organic compounds to multiple chemical mechanisms. *Atmos. Chem. Phys.* 14 (11), 5617–5638. doi:10.5194/acp-14-5617-2014

Li, Z., Yu, S., Li, M., Chen, X., Zhang, Y., Song, Z., et al. (2022). The modeling study about impacts of emission control policies for Chinese 14th five-year plan on $PM_{2.5}$ and O_3 in yangtze river delta, China. *Atmosphere* 13 (1), 26. doi:10.3390/atmos13010026

Liu, C., Zhang, L., Wen, Y., and Shi, K. (2021). Sensitivity analysis of O3 formation to its precursors-Multifractal approach. *Atmos. Environ.* 251, 118275. doi:10.1016/j.atmosenv.2021.118275

Lu, X., Zhang, L., Chen, Y., Zhou, M., Zheng, B., Li, K., et al. (2019). Exploring 2016-2017 surface ozone pollution over China: Source contributions and meteorological influences. *Atmos. Chem. Phys.* 19 (12), 8339–8361. doi:10.5194/acp-19-8339-2019

Luo, H., Zhao, K., Yuan, Z., Yang, L., Zheng, J., Huang, Z., et al. (2021). Emission source-based ozone isopleth and isosurface diagrams and their significance in ozone pollution control strategies. *J. Environ. Sci. (China)* 105, 138–149. doi:10.1016/j.jes.2020.12.033

Ou, J., Yuan, Z., Zheng, J., Huang, Z., Shao, M., Li, Z., et al. (2016). Ambient ozone control in a photochemically active region: Short-term despiking or long-term attainment? *Environ. Sci. Technol.* 50 (11), 5720–5728. doi:10.1021/acs.est.6b00345

Qu, Y., An, J., Li, J., Chen, Y., Li, Y., Liu, X., et al. (2014). Effects of NOx and VOCs from five emission sources on summer surface O3 over the Beijing-Tianjin-Hebei region. *Adv. Atmos. Sci.* 31 (4), 787–800. doi:10.1007/s00376-013-3132-x

Skamarock, W. C., Klemp, J. B., Dudhia, J., Gill, D. O., Zhiquan, L., Berner, J., et al. (2019). A description of the advanced research WRF model version 4. NCAR technical note NCAR/TN-475+STR. AvaliableAt: http://library.ucar.edu/research/publish-technote.

Tan, Z., Lu, K., Jiang, M., Su, R., Dong, H., Zeng, L., et al. (2018). Exploring ozone pollution in chengdu, southwestern China: A case study from radical chemistry to O3-VOC-NOx sensitivity. *Sci. Total Environ.* 636, 775–786. doi:10.1016/j.scitotenv.2018.04.286

Wang, N., Lyu, X., Deng, X., Huang, X., Jiang, F., and Ding, A. (2019). Aggravating O 3 pollution due to NO x emission control in eastern China. *Sci. Total Environ.* 677, 732–744. doi:10.1016/j.scitotenv.2019.04.388

Wickham, J., Stehman, S., Gass, L., Dewitz, J., Sorenson, D., Granneman, B., et al. (2019). EPA public access. *Adv. Ecol. Res.* 60, 1–24. doi:10.1016/j.scitotenv.2019.01.116.Source

Wu, R., and Xie, S. (2017). Spatial distribution of ozone formation in China derived from emissions of speciated volatile organic compounds. *Environ. Sci. Technol.* 51 (5), 2574–2583. doi:10.1021/acs.est.6b03634

Yang, X., Wu, K., Lu, Y., Wang, S., Qiao, Y., Zhang, X., et al. (2021). Origin of regional springtime ozone episodes in the Sichuan Basin, China: Role of synoptic forcing and regional transport. *Environ. Pollut.* 278, 116845. doi:10.1016/j.envpol.2021.116845

Yang, Y., Lan, H., and Li, J. (2020). Spatial econometric analysis of the impact of socioeconomic factors on PM2.5 concentration in China's inland cities: A case study from chengdu plain economic zone. *Int. J. Environ. Res. Public Health* 17 (1), 74. doi:10.3390/ijerph17010074

Yao, S., Wei, W., Cheng, S., Niu, Y., and Guan, P. (2021). Impacts of meteorology and emissions on O_3 pollution during 2013–2018 and corresponding control strategy for a typical industrial city of China. *Atmosphere* 12 (5), 619. doi:10.3390/atmos12050619

Yarwood, G., Emery, C., Jung, J., Nopmongcol, U., and Sakulyanontvittaya, T. (2013). A method to represent ozone response to large changes in precursor emissions using high-order sensitivity analysis in photochemical models. *Geosci. Model Dev.* 6 (5), 1601–1608. doi:10.5194/gmd-6-1601-2013

Yu, S. (2019). Fog geoengineering to abate local ozone pollution at ground level by enhancing air moisture. *Environ. Chem. Lett.* 17 (1), 565–580. doi:10.1007/s10311-018-0809-5

Zhang, W. (2013). Direct sensitivity techniques in regional air quality models: Development and application. Atlanta, Georgia: Georgia Institute of Technology. Doctoral dissertation. Available at: https://smartech.gatech.edu/bitstream/handle/1853/52941/ZHANG-DISSERTATION-2013.pdf?sequence=1&isAllowed=y.

Zhou, Z., Tan, Q., Deng, Y., Wu, K., Yang, X., and Zhou, X. (2019). Emission inventory of anthropogenic air pollutant sources and characteristics of VOCs species in Sichuan Province, China. *J. Atmos. Chem.* 76 (1), 21–58. doi:10.1007/s10874-019-9386-7